

Extraordinary optical transmission through hole arrays in optically thin metal films

Sergio G. Rodrigo,^{1,*} L. Martín-Moreno,¹ A. Yu. Nikitin,^{1,2} A. V. Kats,² I. S. Spevak,² and F. J. García-Vidal³

¹*Instituto de Ciencia de Materiales de Aragón and Departamento de Física de la Materia Condensada, CSIC-Universidad de Zaragoza, E-50009, Zaragoza, Spain*

²*Theoretical Physics Department, A. Ya. Usikov Institute for Radiophysics and Electronics, Ukrainian Academy of Sciences, 12 Academician Proskura Strasse, 61085 Kharkov, Ukraine*

³*Departamento de Física Teórica de la Materia Condensada, Universidad Autónoma de Madrid, Madrid 28049, Spain*

*Corresponding author: sergut@unizar.es

Received July 28, 2008; revised November 6, 2008; accepted November 11, 2008; posted November 18, 2008 (Doc. ID 99422); published December 19, 2008

A theoretical study is presented on the optical transmission through square hole arrays drilled in optically thin films, where transmission may occur through both the holes and the metal layer. It is shown that, as the thickness of the metal film decreases, the coupling of light with short-range surface plasmons redshifts the extraordinary optical transmission peak to longer wavelengths. At the same time, the maximum-to-minimum transmittance ratio is kept high even for metal thicknesses as small as one skin depth. © 2008 Optical Society of America

OCIS codes: 050.1220, 050.1960, 050.6624, 240.6680, 310.6860.

Since the discovery of extraordinary optical transmission (EOT) [1], i.e., resonances in the transmission of light through subwavelength holes drilled in a metal film, numerous works have explored different parameter configurations of two-dimensional hole arrays (2DHAs) [2]. In the now “canonical” configuration [1] the metal film is opaque. In this case, the EOT process involves surface modes at each side of the film that couple through the holes [3]. On the other hand, continuous metal films (thin enough to be translucent), also present transmission resonances when periodically corrugated. In this configuration, resonant spectral features are related to the surface plasmon polaritons (SPPs) of the thin film [4,5], the so-called short-range SPPs (SRs), and the long-range SPPs (LRs) [6].

The transmission of electromagnetic radiation through 2DHA, for thicknesses of the metal film ranging from less than 1 to 2–3 skin depths, has been studied in the terahertz regime [7,8]. These works showed how the intensity of the EOT peak developed with metal thickness, its spectral position being mainly determined by the lattice parameter.

In this Letter, we extend the study to the optical regime. We analyze the optical response of 2DHAs on metal thickness, w , going from optically thick films to films as thin as approximately one “skin depth” (~ 20 nm). This may be of interest in the fields of EOT and negative refractive index (which has been obtained in stacked optically thin 2DHAs [9]). We show that EOT peaks keep a high visibility (defined as the difference between maximum and minimum transmittances divided by the average one) for reasonable hole sizes, a . We find that EOT peaks are due to the excitation of SR resonances; therefore their spectral positions depend strongly on both lattice pa-

rameter and metal thickness. In contrast, LR do not appreciably contribute to transmission spectra.

To provide mechanical stability, actual thin films must lie on a substrate, which we take to be glass. We consider two different dielectric configurations: the asymmetric ($\epsilon_I = \epsilon_{II} = 1.0; \epsilon_{III} = 2.25$) and the symmetric one ($\epsilon_I = \epsilon_{II} = \epsilon_{III} = 2.25$), which can be experimentally obtained by using an index matching liquid. Throughout this Letter we consider square lattices of square holes; the period, P , is chosen to be 400 nm (to obtain EOT in the visible). The metal is gold (with a frequency dependent dielectric constant, ϵ_m taken from [10]). A schematic of the structure is shown as an inset in Fig. 1(c).

Figure 1 renders the computed zero-order transmittance spectra through 2DHAs with different thicknesses for both (a) asymmetric and (b) symmetric configurations. Calculations have been conducted with the finite-difference time-domain (FDTD) method. For optically thick films, the canonical EOT resonant features are observed, which appear at wavelengths slightly redshifted from the Rayleigh wavelength ($\lambda_R = \sqrt{\epsilon_{III}}P = 600$ nm). As the film thickness is reduced, both maximum and minimum transmittance redshifts by even hundreds of nanometers while keeping high peak visibility.

To understand these spectral shifts, we analyze the EM modes bounded to the metal film. A flat unperforated optically thick metal layer supports an SPP on each surface. When the film thickness is reduced, these two modes interact and are substantially coupled whenever the film thickness is smaller than 2–3 skin depths. In this case, the dispersion relations of film modes can greatly differ from that of the SPP, while in the terahertz regime they remain close to the light line. We denote by $\vec{q}_{\text{mode}}(\lambda)$ the in-plane

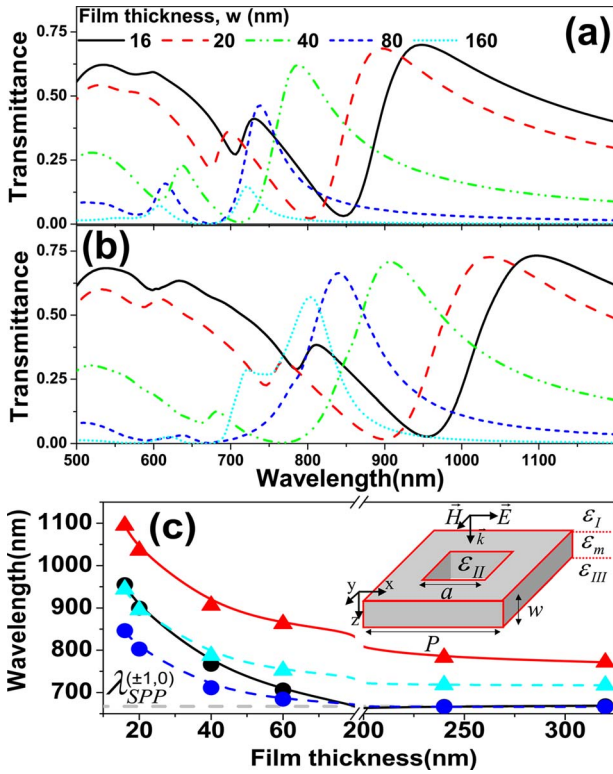


Fig. 1. (Color online) Zero-order transmittance through 2DHAs in gold, as a function of the film thickness ($P=400$ and $a=160$ nm) (a) $\epsilon_I=\epsilon_{II}=1.0$; $\epsilon_{III}=2.25$ and (b) $\epsilon_I=\epsilon_{II}=\epsilon_{III}=2.25$. The spectral position as a function of w for both the EOT maximum (triangular symbols) and the EOT minimum (circular symbols) are shown in panel (c). Dashed curves summarize data obtained from panel (a) while solid curves are used for data taken from panel (b). The horizontal dashed line renders $\lambda_{SPP}^{(\pm 1, 0)}$.

wave vector of these film modes (where the label “mode” can be either SPP, LR, or SR) as a function of the wavelength λ . These film modes couple to external radiation and may lead to transmission resonances that, for small corrugations, are therefore expected to occur close to wavelengths satisfying

$$\left(k_x^{\text{in}} + \frac{2\pi n}{P}\right)^2 + \left(k_y^{\text{in}} + \frac{2\pi m}{P}\right)^2 = q_{\text{mode}}^2(\lambda). \quad (1)$$

Here, the in-plane component of the incident wave vector is $\vec{k}^{\text{in}}=(k_x^{\text{in}}, k_y^{\text{in}})$ and n and m are integers. From now on, we denote by $\lambda_{\text{mode}}^{(n, m)}$ a wavelength that holds Eq. (1) at normal incidence ($\vec{k}^{\text{in}}=0$) for some given values of n and m . Figure 1(c) shows the spectral positions of both minimum and maximum of the EOT peak appearing at the largest wavelengths. We find that when the film is thick enough the EOT minimum very approximately coincides with $\lambda_{SPP}^{(\pm 1, 0)}$ [11]. In contrast, both maximum and minimum redshift as the film thickness reaches the “optically thin” regime.

To analyze whether the EOT phenomenon through optically thin 2DHAs has its origin in the excitation of an EM mode bounded to the film, we focus on the symmetric configuration with $w=20$ nm. Figure 2(a) shows the transmission spectra for 2DHAs with dif-

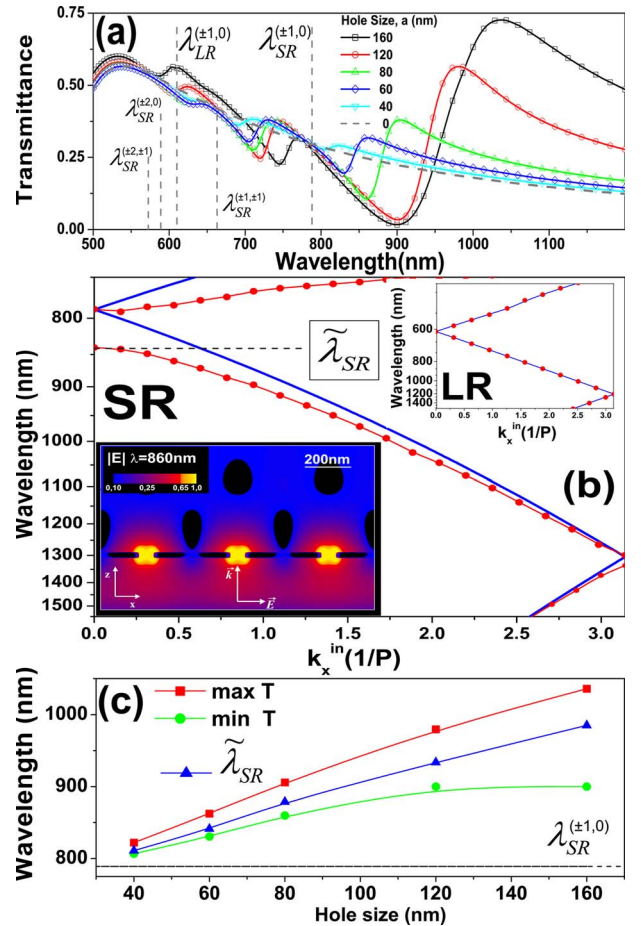


Fig. 2. (Color online) For a holey thin film with $w=20$ nm ($P=400$ nm and $\epsilon_I=\epsilon_{II}=\epsilon_{III}=2.25$), panel (a) shows transmittance versus wavelength for different hole sizes. Vertical dashed curves display several values of $\lambda_{LR}^{(n, m)}$ and $\lambda_{SR}^{(n, m)}$ (see text) at $k_x^{\text{in}}=0$. (b) 2DHA dispersion relations along the x direction for $a=60$ nm (circular symbols). Solid curves represent the folded dispersion relations of LR and SR modes for the unperforated film. The inset in panel (b) shows an $|E|$ field map in the x - z plane ($y=P/2$) at the EOT wavelength. (c) EOT maxima (square symbols), minima (circular symbols), and $\tilde{\lambda}_{SR}$ (triangular symbols) as a function of the hole size.

ferent hole sizes. Vertical dashed lines mark different SR diffracted orders together with $\lambda_{LR}^{(\pm 1, 0)}$. The EOT spectral positions of both maximum and minimum approach $\lambda_{SR}^{(\pm 1, 0)}$ wavelength as the hole size decreases. At the same time, the EOT peak visibility is progressively reduced as the hole size decreases (the dashed curve shows the result for the uniform film). Additionally, there are several small dips in the transmission spectra, which will be discussed later.

To assign even more conclusively EOT features to EM modes of the perforated film, we have calculated the band structure of film modes in the holey film. The result is depicted in Fig. 2(b) (circular symbols) for a 2DHA with $a=60$ nm. The dispersion relations for the bounded modes of a flat film (folded into the first Brillouin’s zone) are represented with continuous curves. As usual, owing to the presence of holes, the modes are coupled at the Brillouin’s zone edges

leading to bandgaps. In the wavelength window shown here, only the mode at the low- λ edge (labeled as $\tilde{\lambda}_{\text{SR}}$) is related to an EOT peak at normal incidence, owing to the structure symmetry [12,13]. The dependence with a hole size of $\tilde{\lambda}_{\text{SR}}$, together with that of the spectral positions of both maximum and minimum transmittance, is displayed in Fig. 2(c). For each hole size $\tilde{\lambda}_{\text{SR}}$ lies between the spectral positions of the transmission maximum and minimum. Nevertheless, as the hole size shrinks to zero, the minimum of transmittance tends to $\tilde{\lambda}_{\text{SR}}$. The inset of Fig. 2(b) renders an $|E|$ field map at the EOT peak wavelength, showing that the field enhancement around the holes [14,15] is also present in optically thin films.

Interestingly, LRs do not noticeably contribute to transmission in the FDTD calculations [Fig. 2(a)]. Notice that, owing to the antisymmetric charge distribution of the LR, its field is almost negligible inside metal and it is less bounded to the surface than an SR mode. Therefore, the LR is both less absorbed and worse coupled to radiation than the SR. In short, the LR field is perturbed very weakly by the holes, so the coupling with the incident light diminishes. A consequence of this is that the LR band structure for the drilled film virtually coincides with the unperforated one [inset Fig. 2(b)].

Therefore, an LR resonance could have been missed given the finite simulation time available. To be sure that LRs are not related to the shallow transmission dips, we have developed an approximate method for solving Maxwell's equations. In this method, the field is represented as a Fourier-Floquet series in the x - y plane and a power series in the coordinate perpendicular to the layer, z [13]. This approach works only for extremely thin metal films, so it has a mainly academic value. Nevertheless, it is useful for understanding the underlying physics. Figure 3 renders transmission spectra calculated with the approximate method for 8 and 10 nm thin films. The zoom in wavelengths close to $\lambda_{\text{LR}}^{(\pm 1,0)}$ (inset in Fig. 3) reveals that extremely narrow peaks can be associated with LR modes. Nevertheless, spectral resolution within the FDTD method does not allow LR peaks to be resolved. The detection of this transmittance peak owing to LR plasmons would be even more difficult from an experimental point of view owing to the finite size of the samples. In any case, this analysis shows that the small dips found with the FDTD method at short wavelengths are exclusively related to higher SR diffracted orders.

In conclusion, we have shown that the EOT peak can be tuned to longer wavelengths (by even hundreds of nanometers) by decreasing the film thickness without strongly affecting either transmission

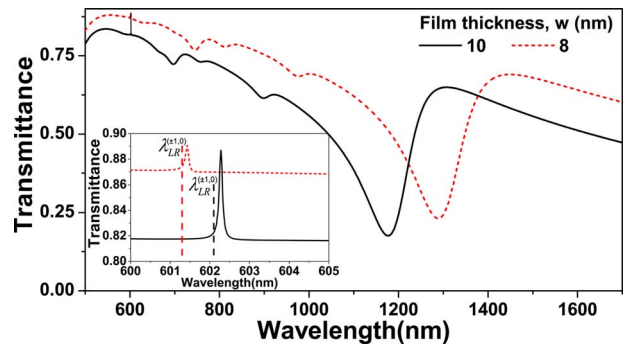


Fig. 3. (Color online) Transmission spectra for two different film widths obtained with the approximate analytical method $w=10$ and $w=8$ nm ($a=160$ nm). Inset, zoom close to the LR wavelengths (corresponding $\lambda_{\text{LR}}^{(\pm 1,0)}$ wavelengths are represented by vertical dashed curves).

intensity or peak visibility (which is still large at $w \sim 20$ nm). We have demonstrated that only SR modes are responsible for the EOT phenomenon in optically thin metallic 2DHAs.

The authors acknowledge financial support from the Spanish Ministry of Science and Innovation under grants MAT2005-06608-C02 and CSD2007-046-NanoLight.es.

References

1. T. W. Ebbesen, H. L. Lezec, H. F. Ghaemi, T. Thio, and P. A. Wolff, *Nature* **391**, 667 (1998).
2. See C. Genet and T. W. Ebbesen, *Nature* **445**, 39 (2007) and references therein.
3. L. Martín-Moreno, F. J. García-Vidal, H. J. Lezec, K. M. Pellerin, T. Thio, J. B. Pendry, and T. W. Ebbesen, *Phys. Rev. Lett.* **86**, 1114 (2001).
4. I. R. Hooper and J. R. Sambles, *Phys. Rev. B* **70**, 045421 (2004).
5. D. Gérard, L. Salomon, F. de Fornel, and A. V. Zayats, *Opt. Express* **12**, 3652 (2004).
6. E. N. Economou, *Phys. Rev.* **182**, 539 (1969).
7. A. K. Azad and W. Zhang, *Opt. Lett.* **30**, 2945 (2005).
8. X. Shou, A. Agrawal, and A. Nahata, *Opt. Express* **13**, 9834 (2005).
9. S. Zhang, W. Fan, N. C. Panoiu, R. M. Osgood, and S. R. J. Brueck, *Phys. Rev. Lett.* **95**, 137404 (2005).
10. E. D. Palik, *Handbook of Optical Constants of Solids* (Academic, 1985).
11. Q. Cao and P. Lalanne, *Phys. Rev. Lett.* **88**, 057403 (2002).
12. S. A. Darmanyan and A. V. Zayats, *Phys. Rev. B* **67**, 035424 (2003).
13. A. V. Kats, M. L. Nesterov, and A. Y. Nikitin, *Phys. Rev. B* **76**, 045413 (2007).
14. L. Salomon, F. D. Grillot, A. V. Zayats, and F. de Fornel, *Phys. Rev. Lett.* **86**, 1110 (2001).
15. A. Krishnan, T. Thio, T. J. Kim, H. L. Lezec, T. W. Ebbesen, P. A. Wolff, J. B. Pendry, L. Martín-Moreno, and F. J. García-Vidal, *Opt. Commun.* **200**, 1 (2001).